

Pore scale consideration in unstable gravity driven finger flow

The Faculty of Oregon State University has made this article openly available.
Please share how this access benefits you. Your story matters.

Citation	Steenhuis, T. S., C. E. Baver, B. Hasanpour, C. R. Stoof, D. A. DiCarlo, and J. S. Selker (2013), Pore scale consideration in unstable gravity driven finger flow, <i>Water Resources Research</i> , 49, 7815–7819. doi:10.1002/2013WR013928
DOI	10.1002/2013WR013928
Publisher	American Geophysical Union
Version	Version of Record
Citable Link	http://hdl.handle.net/1957/47923
Terms of Use	http://cdss.library.oregonstate.edu/sa-termsfuse

Pore scale consideration in unstable gravity driven finger flow

Tammo S. Steenhuis,¹ Christine E. Bayer,¹ Bahareh Hasanpour,¹ Cathelijne R. Stoof,¹ David A. DiCarlo,² and John S. Selker³

Received 4 April 2013; revised 21 October 2013; accepted 22 October 2013; published 22 November 2013.

[2] To explain the dynamic behavior of the matric potential at the wetting front of gravity driven fingers, we take into account the pressure across the interface that is not continuous and depends on the radius of the meniscus, which is a function of pore size and the dynamic contact angle θ_d . θ_d depends on a number of factors including velocity of the water and can be found by the Hoffman-Jiang equation that was modified for gravity effects. By assuming that water at the wetting front imbibes one pore at a time, realistic velocities are obtained that can explain the capillary pressures observed in unstable flow experiments in wettable and water repellent sands.

Citation: Steenhuis, T. S., C. E. Bayer, B. Hasanpour, C. R. Stoof, D. A. DiCarlo, and J. S. Selker (2013), Pore scale consideration in unstable gravity driven finger flow, *Water Resour. Res.*, 49, 7815–7819, doi:10.1002/2013WR013928.

1. Introduction

[3] Fingering flow initiated by gravity has been studied for over 40 years. It is a special case of water infiltration in a porous medium where equilibrium capillary pressure-saturation conditions are not maintained at the wetting front [Hsu and Hilpert, 2011; Mumford and O'Carroll, 2012; DiCarlo 2013]. At the wetting front where fluid saturation changes rapidly, measurements of finger flow behavior by among others Liu *et al.* [1993] and DiCarlo [2004, 2007] show that capillary pressure is a function of the rate of change of saturation, referred to as dynamic capillary pressure [Hsu and Hilpert, 2011]. This discrepancy in predicting wetting front behavior between the static and dynamic approach is especially great when the static contact angle (also called equilibrium contact angle) is intermediate between 0° and 90° [O'Carroll *et al.*, 2010]. The latter might explain why unstable fingering flow is observed in experiments in silica sand with a contact angle between 30° and 60° [Extrand and Kumagai, 1997; Romano, 2006; Schroth *et al.*, 1996] or extremely dry soil [Nektarios *et al.*, 1999].

[4] An agreed upon explanation of the dynamic behavior of the matric potential at the wetting front remains elusive despite investigations by multiple laboratories [O'Carroll *et al.*, 2010]. Most approaches to model the dynamic matric

potential assume that the pressure field at the wetting front is continuous (see DiCarlo 2013, this special issue, for an overview of past approaches). The continuum approach of Hsu and Hilpert [2011] and Hilpert [2012] in which the change in dynamic contact angle and resulting matric potential at the fluid-air interface is related to the velocity of the front seems to be particularly promising. Other modelers employed pore network models that assume that the pressure field can be discontinuous, such that water does not flow through all the pores at the wetting front at the same time [Joekar-Niasar and Hassanizadeh, 2012; DiCarlo, 2013, this special issue]. Very interesting and relevant are findings of Moebius and Or [2012] and Moebius *et al.* [2012] who recorded water moving through pores in packed glass beads with high speed camera and acoustics. They found that all menisci increase in size at the front until water broke through in one pore followed by a decrease in size for all other menisci. Finally, Bayer *et al.* [2013, this special issue] also assumed a discontinuous pressure field at the wetting front.

[5] In the Bayer *et al.* [2013] paper, we argue that the key in explaining finger formation under gravity is that the pressure across the wetting front is discontinuous and determined by the shape of the dynamic (or nonequilibrium) contact angle between the meniscus and the sand grain. Furthermore, we showed that the Hoffman equation relating dynamic contact angle to velocity of moving contact line could be applied in porous media in which gravity was the driving force. By employing a contact line velocity in Hoffman's relationship, we could estimate the matric potential at the wetting front of water moving down in small columns similar to those used in the Geiger and Durnford [2000] experiments with the same precision as Hsu and Hilpert [2011], but with one fitting parameter less because we employed the Hoffman equation. The velocity was calculated by assuming that the imposed flux passed through one or several pores each instant while the other pores had no flow. The two fitting parameters in Bayer *et al.* [2013] were (1) a grain size dependent static contact angle, and (2) the number of pores imbining the imposed flux each

Additional supporting information may be found in the online version of this article.

¹Department of Biological and Environmental Engineering, Cornell University, Ithaca, New York, USA.

²Department of Petroleum and Geosystems Engineering, University of Texas at Austin, Austin, Texas, USA.

³Department of Biological and Ecological Engineering, Oregon State University, Corvallis, Oregon, USA.

Corresponding author: T. S. Steenhuis, Department of Biological and Environmental Engineering, Cornell University, 206 Riley-Robb Hall, Ithaca, NY 14853, USA. (tss1@cornell.edu)

©2013. American Geophysical Union. All Rights Reserved.
0043-1397/13/10.1002/2013WR013928

instant, taken as a function of the quotient of the flux and the saturated conductivity. For a flux of one fifth of the saturated conductivity, only one pore was active each instant to carry the flux downward.

[6] The objective of this study was to validate rigorously the overshoot using the Hoffman equation by using the experiments of *DiCarlo* [2007] in which water was added to small 1.3 cm columns at low rates using the same porous media at three initial moisture contents. Under these low infiltration conditions the water at the finger front is assumed to imbibe one pore at a time and the only adjustable parameter is the static contact angle once the pore neck size is fixed. In addition, we will test the theory using the experiment of *Bauters et al.*'s [1998] that evaluated pressures in fingers moving in water repellent sands.

2. Theory

[7] In well-sorted sands, gravity is the dominant force in unstable fingered flow. Observations show that these gravity driven fingers are more saturated and have a greater matric potential (i.e., negative pressure closer to zero) at the finger tip just behind the wetting front [e.g., *Selker et al.*, 1992]. The term "overshoot," coined by [*DiCarlo*, 2004], is used to describe this phenomenon.

[8] To describe this phenomenon, we will assume that pressure at the wetting front is discontinuous. Then, the capillary pressure at the wetting front of a finger, h (m), is related to the radius of the meniscus that can be expressed through Laplace's equation as:

$$h = -\frac{2\sigma}{\rho g r_m} \left(\frac{1}{r_{m_1}} + \frac{1}{r_{m_2}} \right) \quad (1)$$

where σ is the surface tension (N/m), ρ is the density of the fluid (kg/m^3), g is gravitational constant (m/s^2), and r_{m_1} and r_{m_2} are the axes of the ellipse representing the meniscus (m). Because we have only limited information about the meniscus we will assume that:

$$r_{m_1} = r_{m_2} = r_m \quad (2)$$

[9] In addition, the radius of the meniscus, r_m (m) can be related to the pore radius, r , (m) with aid of the dynamic contact angle θ_d (radians):

$$r_m = \frac{r}{\cos \theta_d} \quad (3)$$

[10] The dynamic contact angle at the wetting front is dependent on the static contact angle, surface tension, viscosity and the velocity of water, and can be found with the Hoffman-Jiang [*Hoffman*, 1975; *Jiang et al.*, 1979] relationship that was modified by *Baver* [2013] and *Baver et al.* [2013, this special issue] who performed experiments that used gravity as:

$$\theta_d = \theta_s + \left(1 - \frac{\theta_s}{\pi} \right) \arccos \left[1 - 2 \tan h(4.96 Ca^{0.702}) \right] \quad (4)$$

where θ_s is the advancing static contact angle (radians) of the water with silica grains and Ca is the dimensionless capillary number defined as:

$$Ca = \frac{\mu V}{\sigma} \quad (5)$$

where μ is the viscosity of the liquid (Pa·s), V is the contact line velocity (m/s), and σ is the surface tension (N/m) between air and water. The contact velocity of the water in the pore can be obtained for small fluxes by assuming that water imbibe pore by pore, and can explain both the dynamic contact angle of the meniscus (equation (3)) and the pressure (equation (1)).

[11] Although the exact velocity of the water flowing through the pore neck is unclear after the meniscus becomes unstable, from a mass balance point of view when water goes down one pore at a time, the average contact line velocity is equal to the flux (Q , m^3/s) in the finger divided by the area of the pore neck. By calculating the velocity this way, we can use equations (1–5) or more detailed in equations (A1)–(A8) in the supporting information to calculate the capillary pressure at the wetting front of the fingertip.

[12] The reasonableness of the assumption of pore-by-pore flow (i.e., one pore at a time) was recently proven by *Mobius and Or* [2012]. With a high speed camera, these investigators measured velocities in pores that were >50 times the average pore diameter. The validity of this one pore at a time assumption can moreover be drawn from the finger flow experiment of *Selker et al.* [1992], where a 0.75 cm variation in the pressure near the wetting front once the tensiometers were fully wetted exceeded that of the pressure variation further behind the front [Figure 8 in *Selker et al.*, 1992]. This pressure variation of 0.75 cm is equivalent to a change in meniscus radius of 20% (!) at the measured fingertip pressure of -3.75 cm. Since the relative change in meniscus radius for the same pressure variation decreases with smaller particle size, this major change in pressures at larger radii could perhaps explain partly why coarse sands are so prone to preferential flow.

3. Application

[13] The theory in section 2 and in the supporting information is tested with the set of experiments reported by *DiCarlo* [2007] and *Bauters et al.* [1998].

3.1. Dry and Moist Sand Experiments by *DiCarlo* [2007]

[14] In *DiCarlo*'s experiments, washed, sieved 20/30 sand (grain size 0.60–0.85 mm, $d_{50} = 0.71$ mm, $K_{\text{sat}} = 15$ cm/min) was packed into slim cylindrical tubes (40 cm long, 1.27 cm inner diameter). Dry sand was premixed with the appropriate amount of water and packed in the column, and pressure was measured with a miniature tensiometer placed 15 cm below the top of the column. Uniform flow rates from 0.001 to 10 cm/min were imposed. Moisture contents were measured in a similar earlier experiment [*DiCarlo*, 2004].

[15] Figure 1 shows the capillary pressure at fingertip for fluxes ranging from 0.001 to 10 cm/min (near-saturated conductivity) for the initially dry sand. The data observed by *DiCarlo* [2007] (Figure 1, symbols) show quite a bit of scatter especially at lower fluxes, that he attributed both to the tensiometer not being well connected at low moisture contents and to random changes in packing. The line in

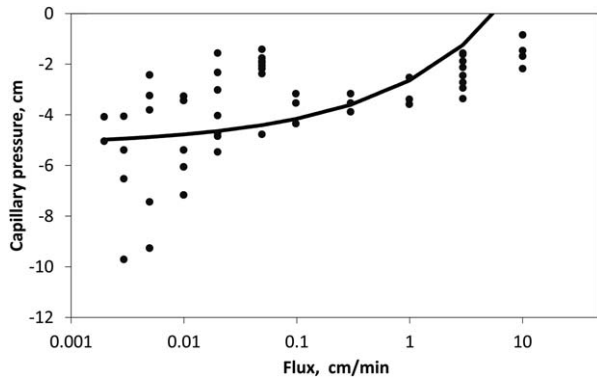


Figure 1. Predicted (line, equations (1–5) and equations (A1)–(A8) supporting information) and observed (symbols) [DiCarlo, 2007] capillary pressure in the fingertip as a function of imposed fluxes in small 1.3 cm wide columns filled with 20/30 sand for the initially dry sand.

Figure 1 illustrates capillary pressures predicted using the characteristics of the porous medium and imbibing liquid in equations (1)–(5) and given in more detail in the supporting information. The pore radius was taken as 0.20 mm, slightly larger than the pore neck radius given by Ng *et al.* [1976] as 21% of the grain diameter, which would correspond to 0.15 mm for the 0.71 mm diameter sand. The static contact angle for the silica sand is between 46° and 56° for the advancing wetting front [Extrand and Kumagai, 1997; Muster *et al.*, 2001; Romano, 2006], we used 50°. Note that the receding contact angle is around 30° [Schroth *et al.*, 1996]. Despite the scatter in the observed data there was a remarkable similar trend of increasing capillary pressure with increasing imposed fluxes ($R^2 = 0.97$) between the observed and the predicted and observed points (Figure 1), with the exception of the pressures at flow rates of 10 cm/min. This is addressed below.

[16] The theory in section 2 can also be applied to the experiments mentioned in the same paper [DiCarlo, 2007] of finger flow through sands at four initial water contents ranging from 0 to 0.14 cm³/cm³ with imposed fluxes ranging from 0.003 to 8.0 cm/min (Tables 1 and 2 and Figure 2, symbols). The predicted capillary pressure (Figure 2, lines) were calculated by using the same parameter values as used for the initially dry sand (Table 1): a pore neck radius of 0.20 mm, and a static contact angle of 50° for the dry sand. We assumed that the static contact angle decreased with increasing initial moisture contents (Table 2). The static contact angle of 20° at 0.14 cm³/cm³ is below that measured by Schroth *et al.* [1996] but may not be unrealistic for wet sand with thick water films. In addition, we

Table 2. Moisture Contents, Static Contact Angles and Measure of Fit (R^2) for Averaged Pressures at Each Moisture Content for the Experiment of DiCarlo *et al.* [2007] Moisture Content (cm³/cm³)

	0	0.03	0.06	0.14
Static contact angle	50	40	30	20
R^2	0.90	0.86	0.88	0.90

adjusted the flow by maximal 35% (see equation (A8) supporting information) to account for initial moisture content in the chamber. The maximum observed (symbols) and predicted capillary pressures (lines) in the finger tips (Figure 2) decrease (become more negative) similarly for decreasing fluxes and for increasing initial water contents. As seen in Figure 1, the predictions shown in Figure 2 are again remarkably close to the observed data with R^2 at or just below 0.9 (Table 2).

[17] The pressure for a flux 10 cm/min in dry sand (Figure 1, and black closed circles in Figure 2) is overpredicted. The flux (10 cm/min) is close to the saturated conductivity of 15 cm/min. As recognized by Parlange and Star [1976], flow becomes stable when the imposed flux is equal to the saturated conductivity. In addition, the overprediction is in agreement with the results of Baver *et al.* [2013], because when fluxes exceed 20% of the saturated conductivity, water flows through more than one pore at the same time reducing the velocity. Lower velocities are related to more negative pressure as is observed in Figure 2.

3.2. Water Repellent Sand Experiments by Bauters *et al.* [1998]

[18] Bauters *et al.* [1998] visualized finger flow during infiltration experiments in slab chambers packed with mixtures of wettable and repellent sand, while measuring pressure heads in the chamber to quantify the flow paths. They used silica sand (0.150–0.840 mm) used in blasting with an average grain diameter of 0.31 mm. The sand was made hydrophobic by coating with octadecyltrichlorosilane (OTS). Between 0.3 and 9.1% of OTS sand was mixed with nonrepellent sand to create sands with varying degrees of repellency ranging from wettable to extremely water repellent. The sand mixtures were poured continuously into the slab chambers (45 cm wide, 57.5 cm tall and 0.8 cm thick). Water was applied evenly along the top of the chamber at a flow rate of 0.4 cm/min. Ponding occurred for all water repellent sands. Pressure in the fingers was measured with fast responding tensiometers and moisture content determined with light intensity (experimental details can be found in Bauters *et al.* [1998]).

Table 1. Experimental Characteristics for the Experiments of DiCarlo [2007] and Bauters *et al.* [1998]

	DiCarlo, Dry Sand	DiCarlo, Wet Sand	Bauters <i>et al.</i> [1998]
Treatment	Dry sand	Several initial moisture contents	Water repellent
Median grain diameter (mm)	0.71	0.71	0.31
Imposed fluxes (cm/min)	0.001–10	0.003–8	0.4
Static contact angle (°)	50	20–50 ^a	50
Pore neck radius (mm)	0.20	0.20	0.09

^aSee Table 2.

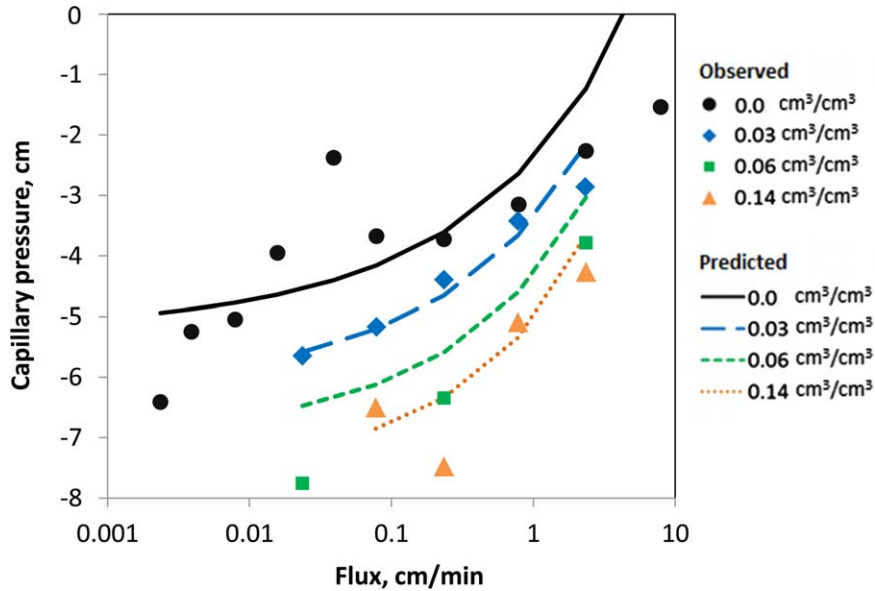


Figure 2. Observed and predicted capillary pressures in the fingertip as a function of moisture content and imposed fluxes. Observed data (symbols) are from infiltration experiments by DiCarlo [2007] in small 1.3 cm wide columns filled with 20/30 sand and are averages over all replicates as each flux. Predicted lines are based on equations (1–5) and equations (A1)–(A8).

[19] Since the water was applied uniformly and sometimes ponded, the imposed flux of 0.4 cm/min is only valid for the uniform wetting front in the hydrophobic sand. For the water repellent sands, the flux was found by invoking the mass balance at the Darcy scale:

$$Q = m_s v_f A_f \tag{6}$$

where m_s is the saturated moisture content, v_f is the finger velocity, and A_f is the cross sectional area of the finger. In addition, we assumed that a small amount of water repellent grains of <10% would not affect overall static contact angle of the sand and was therefore kept at 50°. We also kept the same grain pore neck ratio for the blasting sand as for the 20/30 sand in DiCarlo’s experiment. Finally, the blasting sand was hydrophylic and since unstable flow theory does not apply we used the measured capillary pressure at the wetting front. Using the procedure described in the supporting information and in section 2 with parameters in Table A1 we calculated the capillary pressures at the finger tip with the data in Table 1. The data fit the curve remarkably well (Figure 3) with the assumption that the static contact angle is not affected by the addition of the (few) water repellent grains. The reasons why clearly need further investigation, but is beyond the scope of this note.

[20] In summary, we found that observed dynamic pressures just behind and the dynamic contact angles at the fingertip for dry, moist, and water repellent sand can be predicted with Hoffman’s equation for imposed fluxes that are less than one fifth of the saturated conductivity when the assumptions are made that the pressure at the wetting front is discontinuous and water at the wetting front imbibes one pore at a time, rather than into all pores at the same time. For greater fluxes, more pores imbibe at the same time.

4. Epilogue

[21] In 1972, J-Yves Parlange together with Hill published experimental results of unstable finger flow and 4 years later they solved the finger flow mathematically [Hill and Parlange, 1972]. Although many aspects of unstable flow behind the wetting front were clarified in the past 40 years, a satisfactory physical explanation of the wetting front behavior remained elusive up to now. In the past few years, Parlange insisted that Hoffman’s relationship describing the dynamic contact angle had the ingredients for finding the solution to the wetting front behavior at the finger tip. Although further research is needed, the present paper provides strong evidence that Parlange’s insight was right as we should have expected based on past experience.

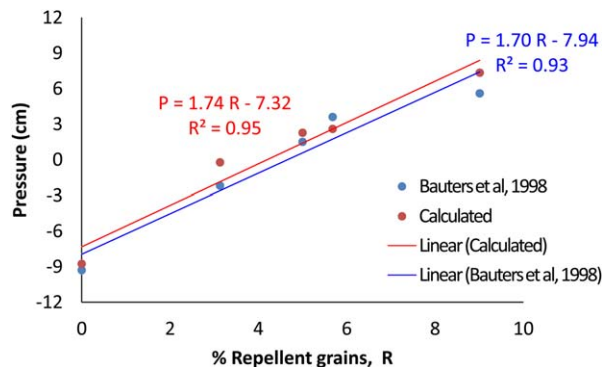


Figure 3. Observed by Bauters *et al.* [1998] and calculated pressures for water infiltrating in water repellent sands with various degrees of water repellencies. Assumption is made that the velocity of the water is equal to calculated flux divided by the radius of the neck.

[22] **Acknowledgments.** NSF provided funding for the organization for the symposium highlighting the work of Parlange and Brutsaert. The discussions during the symposium were the incentive for writing this paper. In addition, we would like to acknowledge the funding from the Binational Agricultural Research and Development Fund (BARD), project IS-3962-07.

References

- Bauters, T. W. J., D. A. DiCarlo, T. S. Steenhuis, and J. Y. Parlange (1998), Preferential flow in water-repellent sands, *Soil Sci. Soc. Am. J.*, *62*(5), 1185–1190.
- Baver, C. E. (2013), Dynamic contact angles and wetting front instability in soils, MS thesis, Biol. and Environ. Eng., Cornell Univ., Ithaca, N. Y. [Available at <http://soilandwater.bee.cornell.edu/publications/ChristineBaverMSThesis.pdf>].
- Baver, C. E., J.-Y. Parlange, C. Stoof, D. DiCarlo, R. Wallach, and T. S. Steenhuis (2013), Dynamic contact angles and wetting front instability, *Water Resour. Res.*, in press.
- DiCarlo, D. A. (2004), Experimental measurements of saturation overshoot on infiltration, *Water Resour. Res.*, *40*, W04215, doi:10.1029/2003WR002670.
- DiCarlo, D. A. (2007), Capillary pressure overshoot as a function of imbibition flux and initial water content, *Water Resour. Res.*, *43*, W08402, doi:10.1029/2006WR005550.
- DiCarlo, D. A. (2013), Unstable multi-phase flow in porous media: 40 years of advancements, *Water Resour. Res.*, doi:10.1002/wrcr.20359, in press.
- Extrand, C. W., and Y. Kumagai (1997), An experimental study of contact angle hysteresis, *J. Colloid Interface Sci.*, *191*, 378–383.
- Geiger, S. L., and D. S. Durnford (2000), Infiltration in homogeneous sands and a mechanistic model of unstable flow, *Soil Sci. Soc. Am. J.*, *64*, 460–469.
- Hill, D. E., and J.-Y. Parlange (1972), Wetting front instability in layered soils, *Soil Sci. Soc. Am. Proc.*, *36*, 697–702.
- Hilpert, M. (2012), Velocity-dependent capillary pressure in theory for variably-saturated liquid infiltration into porous media, *Geophys. Res. Lett.*, *39*, L06402, doi:10.1029/2012GL051114.
- Hoffman, R. L. (1975), Study of advancing interface.1. Interface shape in liquid-gas systems, *J. Colloid Interface Sci.*, *50*, 228–241.
- Hsu, S.-Y., and M. Hilpert (2011), Incorporation of dynamic capillary pressure into the Green-Ampt model for infiltration, *Vadose Zone J.*, *10*, 642–653.
- Jiang, T. S., S. G. Oh, and J. C. Slattery (1979), Correlation for dynamic contact-angle, *J. Colloid Interface Sci.*, *69*(1), 74–77.
- Joekar-Niasar, V., and S. M. Hassanizadeh (2012), Analysis of fundamentals of two-phase flow in porous media using dynamic pore-network models: A review, *Crit. Rev. Environ. Sci. Technol.*, doi: 10.1080/10643389.2011.574101.
- Liu, Y., B. R. Bierck, J. S. Selker, T. S. Steenhuis, and J.-Y. Parlange (1993), High-intensity X-ray and tensiometer measurements in rapidly changing preferential flow fields, *Soil Sci. Soc. Am. J.*, *57*, 1188–1192.
- Moebius, F., and D. Or (2012), Interfacial jumps and pressure bursts during fluid displacement in interacting irregular capillaries, *J. Colloid Interface Sci.*, *377*, 406–415.
- Moebius, F., D. Canone, and D. Or (2012), Characteristics of acoustic emissions induced by fluid front displacement in porous media, *Water Resour. Res.*, *48*, W11507, doi:10.1029/2012WR012525.
- Mumford, K. G., and D. M. O’Carroll (2012), Drainage under nonequilibrium conditions: Exploring wettability and dynamic contact angle effects using bundle-of-tubes simulations, *Vadose Zone J.*, *10*, 1162–1172.
- Muster, T. H., C. A. Prestidge, and R. A. Hayes (2001), Water adsorption kinetics and contact angles of silica particles, *Colloids Surf. A*, *176*(2–3), 253–266.
- Nektarios, P. A., T. S. Steenhuis, A. M. Petrovic, and J.-Y. Parlange (1999), Fingered flow in laboratory golf putting greens, *J. Turfgrass Manage.*, *3*, 53–67.
- Ng, K. M., H. T. Davis, and L. E. Scriven (1978) Visualization of blob mechanics in flow through porous media, *Chem. Eng. Sci.*, *33*, 1009–1017.
- O’Carroll, D. M., K. G. Mumford, L. M. Abriola, and J. I. Gerhard (2010), Influence of wettability variations on dynamic effects in capillary pressure, *Water Resour. Res.*, *46*, doi:10.1029/2009WR008712.
- Parlange, J.-Y., and D. Hill (1976), Theoretical analysis of wetting front instability in soils, *Soil Sci.*, *122*(4), 236–239.
- Romano, R. J. (2006), Contact angles, 2006 REU Program, Cent. for High Rate Nanomanuf., Univ. of Mass. Lowell. [Available at http://www.northeastern.edu/chn/education_outreach/research_education/reu_program/reu_2006/documents/Romano.pdf].
- Schroth, M. H., S. J. Ahearn, J. S. Selker, and J. D. Istok (1996), Characterization of miller-similar silica sands for laboratory hydrologic studies, *Soil Sci. Soc. Am. J.*, *60*(5), 1331–1339.
- Selker, J. S., T. S. Steenhuis, and J.-Y. Parlange (1992), Wetting front instability in homogeneous sandy soils under continuous infiltration, *Soil Sci. Soc. Am. J.*, *56*(5), 1346–1350.